Metal-Enhanced Phosphorescence: Interpretation in Terms of Triplet-Coupled Radiating Plasmons

Yongxia Zhang,[†] Kadir Aslan,[†] Michael J. R. Previte,[†] Stuart N. Malyn,[†] and Chris D. Geddes*,[‡]

Institute of Fluorescence, Laboratory for Advanced Medical Plasmonics, Medical Biotechnology Center, University of Maryland Biotechnology Institute, 725 West Lombard Street, Baltimore, Maryland 21201, and Center for Fluorescence Spectroscopy, Department of Biochemistry and Molecular Biology, Medical Biotechnology Center, University of Maryland School of Medicine, 725 West Lombard Street, Baltimore, Maryland 21201

We report our detailed metal-enhanced phosphorescence (MEP) findings using Rose Bengal at low temperature. Silver Island Films (SiFs) in close proximity to Rose Bengal significantly enhance the phosphorescence emission intensity. In this regard, a 5-fold brighter phosphorescence intensity of Rose Bengal was observed from SiFs as compared to a glass control sample at 77 K. In addition, several factors affecting MEP, such as distance dependence and silver film morphology, were also investigated. Our findings suggest that both singlet and triplet states can couple to surface plasmons and enhance both fluorescence and phosphorescence yields. This finding suggests that MEP can be used to promote triplet-based assays, such as those used in photodynamic therapy.

1. Introduction

Photodynamic therapy (PDT) has potential in the diagnosis and treatment of several diseases such as diabetes, peripheral vascular diseases, cerebrovascular, and cardiovascular.[1] As early as the end of last century, PDT was first used for the treatment of skin cancers and paramecia.[2] Since then, many kinds of cancers (lung, colon, etc.) as well as certain kinds of blindness have been dealt with using PDT. More recently, PDT has been used for photorejuvenation, wrinkles, discoloration, visible veins, and acne.[3] In all PDT treatments, the main focus is on inducing cell death when a suitable dye (lumophore), light, and oxygen are combined. There are several notable advantages of PDT treatments; for example, they are less destructive (and therefore less painful) and typically need less recovery time than many other treatments.

Three primary processes are known to be involved in the photodynamic effect: First, the ground state of the dye (S_0) is optically excited to an excited singlet state. Next, a population from the excited state is typically transferred to the dye's lowest triplet state by intersystem crossing. Finally, collisional energy transfer from the triplet dye to ground-state molecular oxygen ($^3O_2$) produces highly reactive singlet oxygen, returning the dye to its original ground state. The singlet oxygen can react readily with many biological targets and destroy a wide variety of cells. However, modern PDT is limited by an insufficient quantity of singlet oxygen, while reacting with biological targets.[1,4] Because singlet oxygen plays a very important role for cell damage, an abundant supply of oxygen is very important. If the consumption of oxygen by the photodynamic process is faster than it can be resupplied, it causes oxygen depletion. An alternative method to resolve this problem is to populate high-lying triplet excited

states of several dyes that produce oxygen-independent damage.[4] If these excited triplet states obtain sufficient energies to allow for the cleavage of one of the molecular bonds, then radicals that are even more reactive than singlet oxygen can be produced. The production of these radicals does not require the presence of oxygen. Yet both mechanisms, that is, $^1O_2$ and radical, do require high phosphorescence (triplet) quantum yields.

In recent years, our laboratories have both introduced and demonstrated many applications of metal-enhanced fluorescence (MEF),[5–7] metal-enhanced chemiluminescence,[8] and indeed surface plasmon coupled fluorescence.[9] These have included the increased detectability and photostability of fluorophores[5–7,10–11] and chemiluminescent species,[8] improved DNA detection,[12] the release of self-quenched fluorescence of over-labeled proteins,[13] enhanced wavelength-ratiometric sensing,[14] and the application of metallic surfaces to ultrafast and ultrasensitive target analyte detection.[15] Our current interpretation of MEF is shown in Figure 1, top: nonradiative energy transfer occurs from excited distal fluorophores to the surface plasmon electrons on noncontinuous films. The surface plasmons in turn radiate the photophysical characteristics of the coupling fluorophores.[16] This explanation has been facilitated by our recent finding of surface plasmon coupled emission (SPCE),[18] whereby fluorophores distal to a continuous metallic film can directionally radiate fluorophore emission at a unique angle from the back of the film. Remarkably, the plasmon coupled emission is completely p-polarized, irrespective of the excitation polarization.[9,17]

We have recently reported the first observation of metal-enhanced phosphorescence[19] (MEP) in a short letter, where nonradiative energy transfer occurs from excited distal lumi-nophores to the surface plasmon electrons in noncontinuous silver films, which in turn radiate Rose Bengal emission efficiently (Figure 1, bottom).

In this paper, we report our detailed MEP findings using Rose Bengal (RB). The phosphorescence intensity is ~5-fold brighter

* Corresponding author. E-mail: geddes@umbi.umd.edu.
† University of Maryland Biotechnology Institute.
‡ University of Maryland School of Medicine.

Metal-Enhanced Phosphorescence

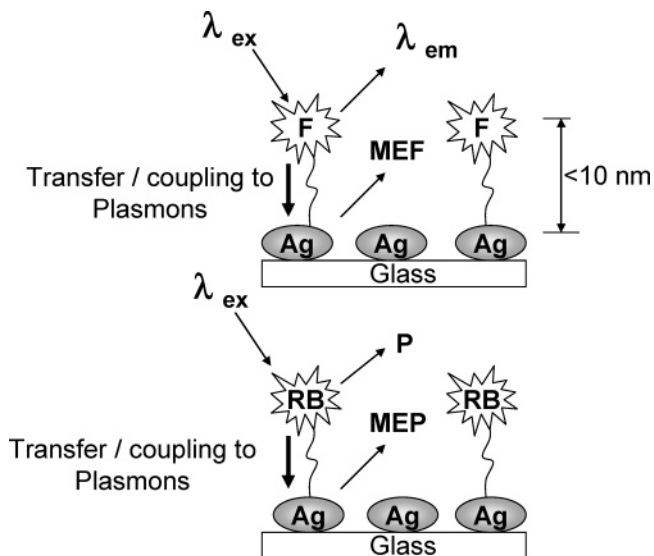*J. Phys. Chem. B, Vol. 110, No. 49, 2006* **25109**

Figure 1. Graphical representation of metal-enhanced fluorescence (top), and of metal-enhanced phosphorescence (bottom). F, fluorophore; RB, Rose Bengal; P, phosphorescence; and MEP, metal-enhanced phosphorescence.

from Silver Island Films (SiFs) as compared to glass, a control sample also at 77 K. In addition, several other factors influencing MEP, such as distance dependence from the surface, silver film morphology, and spin−orbital coupling, are also studied. This observation is not only helpful in our understanding of plasmon−luminophore interactions, but suggests that this approach may be of significance for phosphorescence triplet state-based clinical assays such as those used in PDT, where high triplet yields are preferred.

2. Experimental Section

Silver nitrate (99.9%), sodium hydroxide (99.996%), ammonium hydroxide (30%), D-glucose, premium quality silane-prep glass slides (75 × 25 mm), silver foil (0.05 mm thick, 99.9%), and ethanol (HPLC/spectrophotometric grade) were obtained from Sigma-Aldrich. All chemicals were used as received.

2.1. Methods. *Preparation of Silver Island Films (SiFs).* SiFs were prepared as we have previously published.[15] In a typical SiFs preparation, a solution of silver nitrate (0.5 g in 60 mL of deionized water) was put in a clean 100-mL glass beaker. 200 μL of freshly prepared 5% (w/v) sodium hydroxide solution and 2 mL of ammonium were added to a continuously stirred silver nitrate solution at room temperature. Subsequently, the solution was cooled to 5 °C by placing the beaker in an ice bath, followed by soaking the silane-prep glass slides in the solution and adding a fresh solution of D-glucose (0.72 g in 15 mL of water). The temperature of the mixture was then allowed to warm to 30 °C. As the color of the mixture turned from yellow green to yellowish brown, the slides were removed from the mixture, washed with water, and sonicated for 1 min at room temperature.

Preparation of the Sandwich Format Sample. 300 μL of Rose Bengal (1.0 × 10⁻⁴ M) in ethanol solution was trapped in a sandwich format between the glass slides and the silver island films, respectively. Figure 2, bottom inset, shows the experimental sample geometry. The glass/SiFs surfaces were placed in liquid nitrogen for 2 min and used for the low-temperature (77 K) measurements.

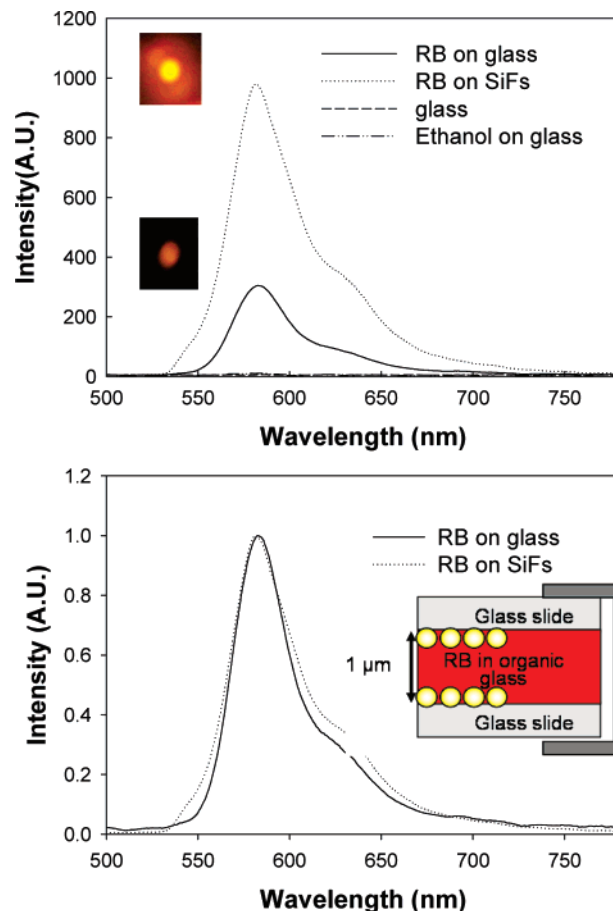*Preparation of Dried Sample on Surface.* 300 μL of Rose Bengal (1.0 × 10⁻⁴ M) in ethanol solution was dropped on the

Figure 2. Fluorescence emission spectra, $\lambda_{ex} = 532$ nm, of Rose Bengal sandwiched between two silvered and unsilvered slides at room temperature (top), and the normalized emission spectra from both glass and silver (bottom). Sandwich experimental geometry (bottom inset).

surfaces of glass, SiFs, and silver foil. The solvent was evaporated, and the samples were studied.

Absorption, Fluorescence, and Phosphorescence Measurements. Absorbance spectra were taken using a Varian Cary 50 UV−vis spectrophotometer. Fluorescence and phosphorescence collection measurements were performed at 45° to the excitation, through a long pass filter, using a fiber optic spectrometer (HD2000) from Ocean Optics, Inc. Phosphorescence excitation spectra were measured using a Cary Eclipse fluorescence spectrophotometer.

Luminescence Lifetime Analysis. Fluorescence lifetimes were measured using the time-correlated single photon counting technique, a PicoQuant modular fluorescence lifetime spectrometer (Fluo Time 100) with a PicoQuant 497 nm LED (PLS-8-2-1015) as the light source. The intensity decays were analyzed in terms of the multiexponential model:

$$I(t) = \sum_i \alpha_i \exp(-t/\tau_i) \tag{1}$$

where α_i are the amplitudes and τ_i are the decay times, $\sum_i \alpha_i = 1.0$. The fractional contribution of each component to the steady-state intensity is given by:

$$f_i = \frac{\alpha_i \tau_i}{\sum_j \alpha_j \tau_j} \tag{2}$$

The mean lifetime of the excited state is given by:

$$\bar{\tau} = \sum_i f_i \tau_i \qquad (3)$$

and the amplitude-weighted lifetime is given by:

$$\langle \tau \rangle = \sum_i \alpha_i \tau_i \qquad (4)$$

The values of α_i and τ_i were determined by a nonlinear least-squares impulse reconvolution with a goodness-of-fit X^2 criterion.

Phosphorescence lifetimes were recorded using a Cary Eclipse fluorescence spectrophotometer and off-gated detection.

3. Results and Discussion

Because of the possible occurrence of multiple phenomena at the same time in the same system in the study of metal-enhanced phosphorescence from Rose Bengal, such as metal-enhanced fluorescence, metal-enhanced phosphorescence, enhanced absorption, reverse intersystem crossing, and spin−orbit coupling, this section was divided into subsequent subsections describing each eventuality.

3.1. Metal-Enhanced Fluorescence. Figure 2, top, shows the fluorescence emission spectra, $\lambda_{ex} = 532$ nm, for Rose Bengal sandwiched between two glass and silvered slides at room temperature. We can see that the enhanced fluorescence intensity was >3-fold brighter from the silver, as compared to glass (978 vs 303 A.U.), where both spectra are identical when normalized (Figure 2, bottom). In our previous studies,[5−7] the MEF phenomenon has reported enhancements of between 2- and 10-fold using similar SiFs geometries. However, the true MEF enhancement factor is actually larger than 3 and is indeed ~75-fold. This is because the MEF phenomenon is a distance-dependent phenomenon coupling to the surface plasmons up to about 10 nm from the surface.[24] With a sample thickness of 1 μm, then only 4% of the sample is within the effective MEF enhancement region, and hence the true enhancement factor is approximately 25 times larger. The photograph inset also shows that the emission intensity is much more clearly detectable from between SiFs than from the glass control slide.

In addition to close proximity nanostructures, there are other factors that can affect the magnitude of the MEF phenomenon, such as temperature. It can be expected that if all other factors remain constant, the quantum efficiency of fluorescence will decrease with increasing temperature.[26] Figure 3 shows the fluorescence emission spectra of Rose Bengal from between the SiFs and from glass at 77 K. It can be seen that the enhanced fluorescence intensity was >5-fold brighter from silver as compared to the glass control sample.

3.2. Metal-Enhanced Phosphorescence. Metal-enhanced phosphorescence (MEP) of Rose Bengal on SiFs was studied, Figure 4, also at low temperature. Phosphorescence is not readily observed at room temperature because of collisional deactivation by oxygen and the presence of quenching impurities.[26] Phosphorescence signals can, however, be observed at low temperatures and in media where the diffusion of both the luminophore and the oxygen is negligible, such as in organic glasses as reported here. From Figure 4, the enhanced phosphorescence intensity was ~5-fold brighter from the silver, as compared to glass (497 vs 110 A.U.), and both spectra are identical when normalized (data not shown). The photograph insets of Figure 4 also show the enhanced phosphorescence visibly from both glass and SiFs. The emission intensity is clearly detectable from between the SiFs, but much weaker from the glass control slide. Table 1 summarizes the fluorescence and phosphorescence
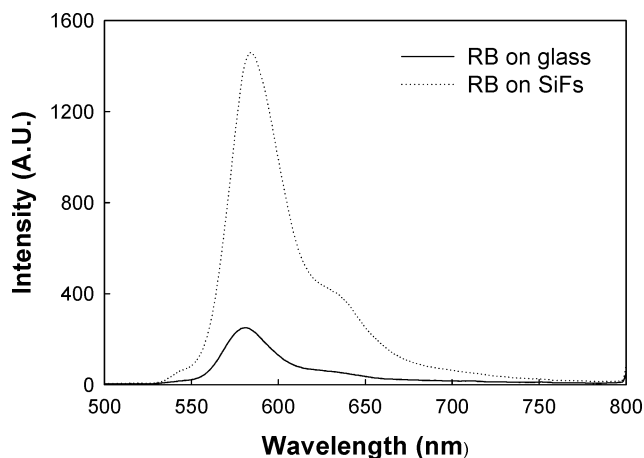

Figure 3. Fluorescence emission spectra of Rose Bengal at 77 K between both silvered and unsilvered glass slides. $\lambda_{ex} = 532$ nm.
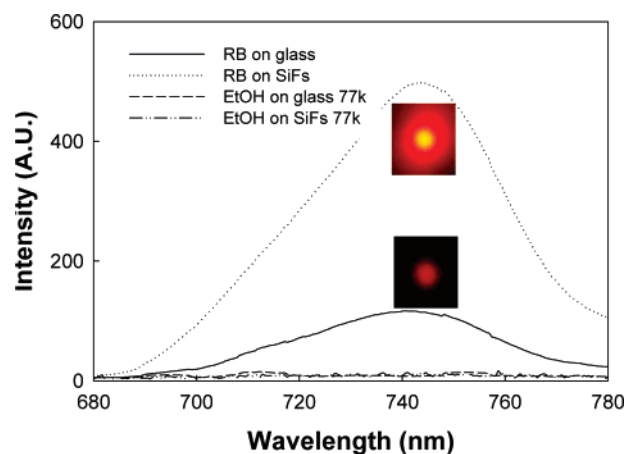

Figure 4. Phosphorescence spectra of Rose Bengal immobilized in an organic glass from between both silvered and unsilvered glass slides at 77 K. $\lambda_{ex} = 532$ nm.

spectral data for Rose Bengal at RT and 77 K sandwiched between both glass and silver slides. It can be seen that the Rose Bengal MEF enhancement ratio increases from 3.2 (at room temperature) to 5.7 (at 77 K). The full-width at half-maximum (fwhm) values of fluorescence and phosphorescence spectral data for Rose Bengal at RT and 77 K are also shown in Table 1. The fwhm for the fluorescence emission spectra at RB on SiFs of 77 K was 38 nm, which is narrower as compared to that measured at room temperature (~44 nm). As expected, the emission maxima wavelength at 77 K is identical to that of the spectra measured at room temperature.

At first consideration, one may be surprised by the presence of both MEP and MEF in the same system as both processes are effectively competitive, both providing for deactivation of electronic excited states. As described in the introduction, and indeed shown in Figure 1, top, MEF is currently thought to occur due to the efficient nonradiative transfer to surface plasmons (a surface mirror dipole), which, in turn, efficiently radiate the photophysical characteristics of the fluorophore. For MEP, a similar process is also thought to occur as depicted by Figure 1, bottom. Similarly, our group has also recently shown that chemiluminescence species, which are electronically excited as the result of a chemical reaction, can also be plasmon enhanced by the presence of silver nanostructures, metal-enhanced chemiluminescence (MEC).[8] At present, we have two possible explanations for the occurrence of both MEF and MEP in the same system: (1) enhanced net system absorbance, which would increase the net singlet and triplet yields, and (2) reverse

TABLE 1: Fluorescence and Phosphorescence Spectral Data for Rose Bengal at Room Temperature and 77 K Sandwiched between Both Glass and Silvered Slides[a]

	fluorescence		phosphorescence
	fwhm (nm)	enhancement factor (integrated area ratio)	enhancement factor (integrated area ratio)
Rose Bengal glass slides, RT	37.4		
Rose Bengal glass slides, 77 K	33.2		
Rose Bengal SiFs, RT	44.1	3.2 (3.6)	
Rose Bengal SiFs, 77 K	38.1	5.7 (5.8)	4.2 (6.5)

[a] The enhancement factor was calculated as the "peak" emission intensity ratio SiFs/glass. Integrated area ratio is the ratio of the area under the fluorescence and phosphorescence spectra on SiFs and glass. fwhm, full-width at half-maximum.
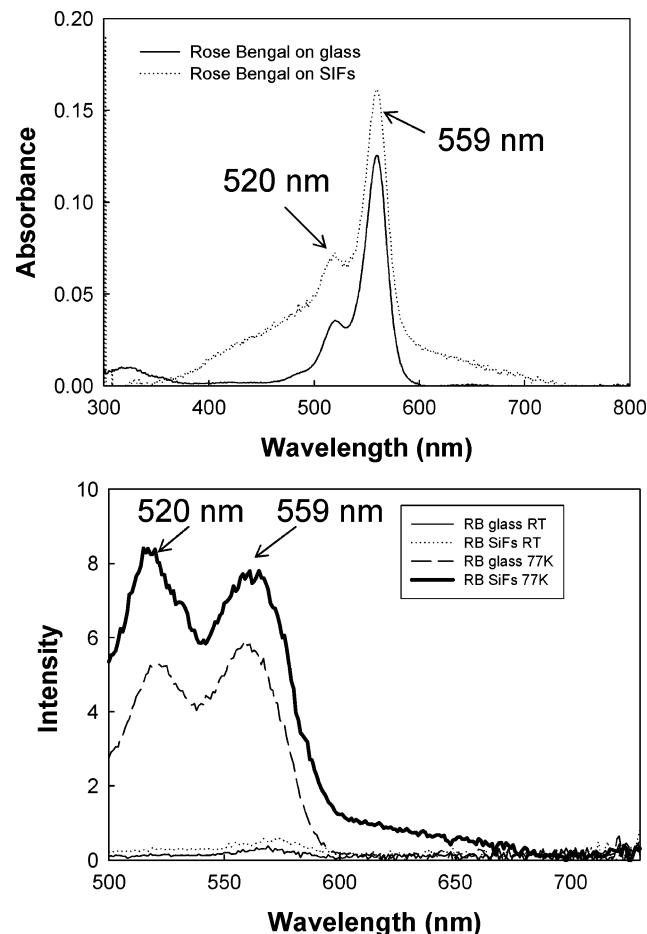

Figure 5. Absorption spectra of Rose Bengal immobilized in an organic glass, sandwiched between two silvered and unsilvered slides, respectively (top), and the phosphorescence excitation spectrum (bottom). $\lambda_{em} = 740$ nm.

intersystem crossing, that is, $T_n \rightarrow S_n$, where the triplet state is populated and the back intersystem crossing facilitates MEF.

3.2.1. Enhanced Absorption. In this regard, we studied the absorption of Rose Bengal in the presence and absence of SiFs. Figure 5, top, shows the absorption spectra of Rose Bengal solution immobilized in an organic glass with and without SiFs. SiFs and glass without Rose Bengal were used as reference backgrounds for the Rose Bengal absorption measurements, respectively. It can be seen that the Rose Bengal has a much larger absorbance on SiFs as compared to that on glass. These effects can be explained as a result of the coupling of the molecular dipoles with the localized electromagnetic field of the metallic particle's surface plasmon resonance (localized plasmon resonance, LPR).[7] In essence, conducting metallic particles can modify the free-space absorption condition (observed in the absence of metal) in ways that increase the incident

electric field, Em, felt by Rose Bengal.[10] From Figure 5, top, it also can be observed that the adsorption spectrum of Rose Bengal on SiFs does not show a simple superpositioning of SiFs and Rose Bengal absorption spectrum, where the SiFs absorption is blanked as a background. The absorption spectrum of Rose Bengal from between the SiFs shows significant broadening as compared to that on glass. This broadening is thought due to the strong overlap of the surface plasmon resonance of SiFs (LPR) and the dipole of Rose Bengal, that is, an enhanced excitation rate.[10,20]

Figure 5, bottom, shows the phosphorescence excitation spectra of Rose Bengal (77 K) immobilized in an organic glass sandwiched between two silvered and unsilvered slides, respectively. From the figure, we can see the same excitation bands as the absorption spectra (Figure 5, top), that is, 520 and 559 nm, respectively. While the ratio of the bands is different, this similarity suggests a singlet absorption followed by $S_n \rightarrow T_n$ intersystem crossing, the $T_1 \rightarrow S_0$ phosphorescence enhanced by the initial enhanced $S_0 \rightarrow S_n$ absorption, and the subsequent greater likelihood of more intersystem crossing. Of course, the metal could also modify the intersystem crossing rate, but we have no direct evidence for this and our Radiating Plasmon Model[20] has not been modified to account for this at this time. It therefore seems reasonable that net system absorption would facilitate both MEP and MEF simultaneously, as we have observed, Figures 2−5.

3.2.2. Reverse Intersystem Crossing. Alternatively, Rose Bengal is known to undergo reverse intersystem crossing or sometimes called back intersystem crossing, which is the inverse of the more-common S_n–T_n intersystem crossing.[26] For possible enhanced direct triplet absorption (from Figure 5, bottom), the MEF and MEP processes for Rose Bengal may not be competing but more likely are complimentary processes, especially if the singlet and triplet energy levels are similar at low temperature. In this case, it seems reasonable that both states, S_1 and T_1, could both induce and couple to surface plasmons as has been observed many times by our laboratory for enhanced S_1 emission at room temperature.[5−7]

While we see no direct evidence for a direct triplet absorption in Figure 5, we subsequently measured the fluorescence and phosphorescence lifetimes, Tables 2, 3, and Figure 6, to investigate whether a much longer fluorescence lifetime, indicative of back intersystem crossing, was evident.

3.3. Fluorescence and Phosphorescence Lifetimes. From Table 2, we can see that the amplitude-weighted lifetime $\langle \tau \rangle$ for Rose Bengal in a cuvette is much shorter at RT (0.75 ns) as compared to that measured at 77 K (1.12 ns). This result is expected and is simply explained by the lack of quenching at reduced temperatures and/or reduced nonradiative rates.[26] This increase in lifetime is also mirrored from the glass sandwich geometries, that is, 0.67 ns for glass at RT and 1.03 ns for glass at 77 K. This trend is also evident on Silver Island Films at RT and 77 K, but the amplitude-weighted lifetimes are shorter (0.68

TABLE 2: Fluorescence Intensity Decay Analysis[a]

	τ_1 (ns)	α_1 %	τ_2 (ns)	α_2 %	τ_3 (ns)	α_3 %	$\langle\tau\rangle$ ns	$\bar{\tau}$ (ns)	χ^2
RB in cuvette RT	0.50	35.2	0.87	64.7	9.3	0.05	0.75	0.67	0.88
RB in cuvette 77 K	1.12	99.8	8.40	0.02			1.12	1.32	0.87
RB on glass RT	0.55	99.3	18.7	0.66			0.67	3.88	1.02
RB on glass 77 K	0.77	96.1	3.30	0.29	2.59	0.98	1.03	7.16	1.01
RB on SiFs RT	0.65	98.4	2.39	1.19	21.5	0.34	0.68	0.96	1.03
RB on SiFs 77 K	0.60	95.9	2.49	3.19	24.4	0.82	0.86	6.33	1.07

[a] $\bar{\tau}$, mean lifetime; $\langle\tau\rangle$, amplitude-weighted lifetime.

TABLE 3: Phosphorescence Intensity Decay Analysis[a]

	τ (ms)	χ^2
RB glass, 77 K	0.31	0.99
RB SiFs, 77 K	0.24	0.99

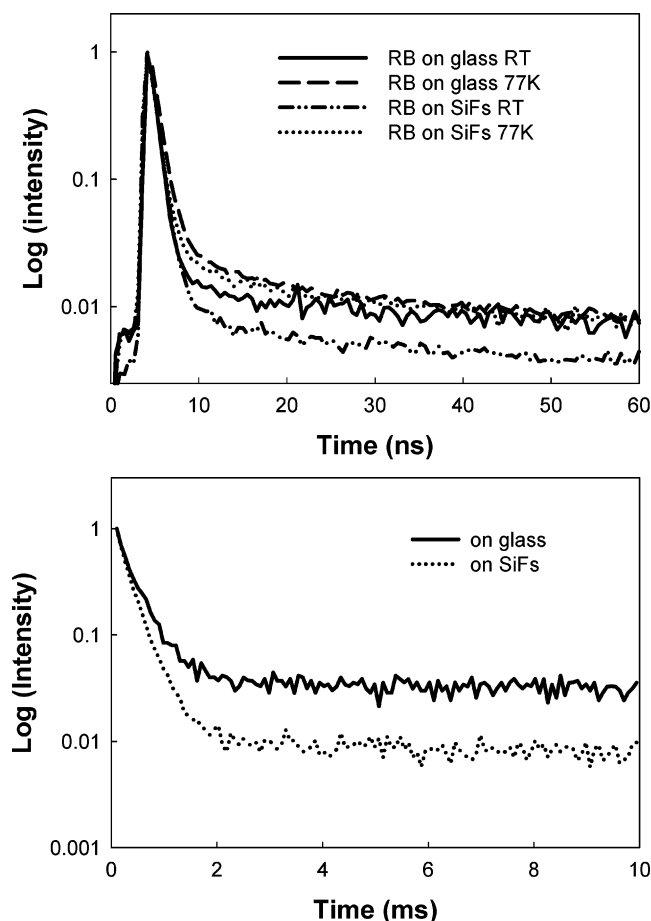[a] The fitting model used to describe the data was: $I(t) = \exp(-t/\tau) + c$.

Figure 6. Fluorescence intensity decays of RB between silvered and unsilvered glass slides at both room temperature (RT) and 77 K (top). Phosphorescence intensity decay at 77 K (bottom).
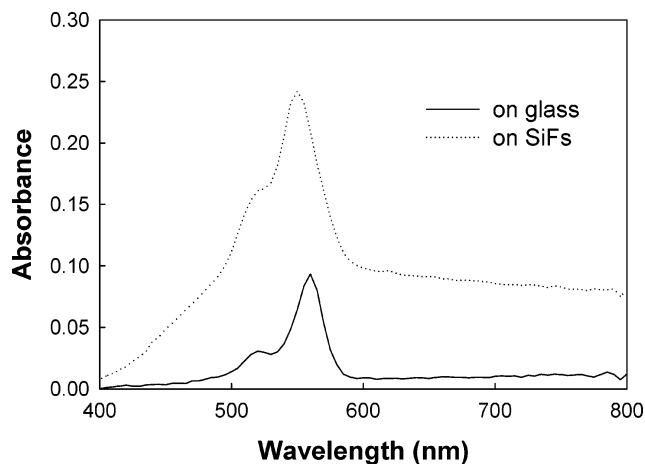

Figure 7. Absorption spectra of Rose Bengal directly dried onto both glass and silvered glass. Glass and SiFs without Rose Bengal were used as blanks, respectively.

and 0.86 ns, respectively). Similarly, the recovered phosphorescence lifetime for RB is also shorter in the presence of silver, that is, 0.31 ms on glass (77 K) versus 0.24 ms on SiFs (77 K), Table 3. Given that only slight increases in fluorescence lifetime are observed at 77 K, coupled with the fact that no evidence for direct triplet absorption is evident, then the occurrence of both MEF and MEP in the same system looks likely to be due to a net increase in system absorption, cf., Figure 5.

The fluorescence and phosphorescence intensity decays can be seen in Figure 6. These decays were used to calculate the respective lifetimes shown in Tables 2 and 3 using nonlinear least-squares regression analysis.[26] From Figure 6 and Tables 2 and 3, we can see a reduced lifetime for fluorophores near-to silver as compared to the glass control sample. In fact, shorter lifetimes for fluorophores/luminophores in close proximity to silver nanostructures coupled with enhanced emission intensities in the same system is indicative of the MEF phenomenon, and has been both reported and explained by our group many times previously.[5,20] This can be understood from the following set of equations.

In fluorescence, the spectral observables are governed by the magnitude of Γ, the radiative decay rate, relative to the sum of the nonradiative decay rates, k_{nr}, such as internal conversion and quenching. In the absence of metallic particles or surfaces, then the quantum yield Q_0 and fluorescence lifetime τ_0 are given by:

$$Q_0 = \frac{\Gamma}{\Gamma + k_{nr}} \tag{5}$$

$$\tau_0 = \frac{1}{\Gamma + k_{nr}} \tag{6}$$

Fluorophores with high radiative rates have high quantum yields and short lifetimes. Increasing the quantum yield requires decreasing the nonradiative rates k_{nr}, which is often only accomplished when using low solution temperatures or a fluorophore binding in a more rigid environment.[26] The natural lifetime of a fluorophore, τ_N, is the inverse of the radiative decay rate or the lifetime that would be observed if their quantum yield were unity. This value is determined by the oscillator strength (extinction coefficient) of the electronic transition.[20] The extinction coefficients of chromophores are only very slightly dependent on their environment. Hence, for almost all examples currently employed in fluorescence spectroscopy today, the radiative decay rate is essentially constant.

Metal-Enhanced Phosphorescence

J. Phys. Chem. B, Vol. 110, No. 49, 2006 **25113**

TABLE 4: Fluorescence and Phosphorescence Spectral Data for Rose Bengal at Room Temperature and 77 K Dried Directly onto Both Glass and Silvered Slides[a]

Rose Bengal dried on surface	fluorescence		phosphorescence
	fwhm (nm)	enhancement factor (integrated area ratio)	enhancement factor (integrated area ratio)
Rose Bengal glass slides, RT	55.3		
Rose Bengal glass slides, 77 K	41.8		
Rose Bengal SiFs, RT	54.2	5.4 (4.0)	
Rose Bengal SiFs, 77 K	49.9	16.5 (13.1)	2.3 (2.1)

[a] The enhancement factor was calculated as the "peak" emission intensity ratio SiFs/glass. The integrated area ratio is the ratio of the area under the fluorescence and phosphorescence spectra on SiFs and glass, respectively. fwhm, full-width at half-maximum.
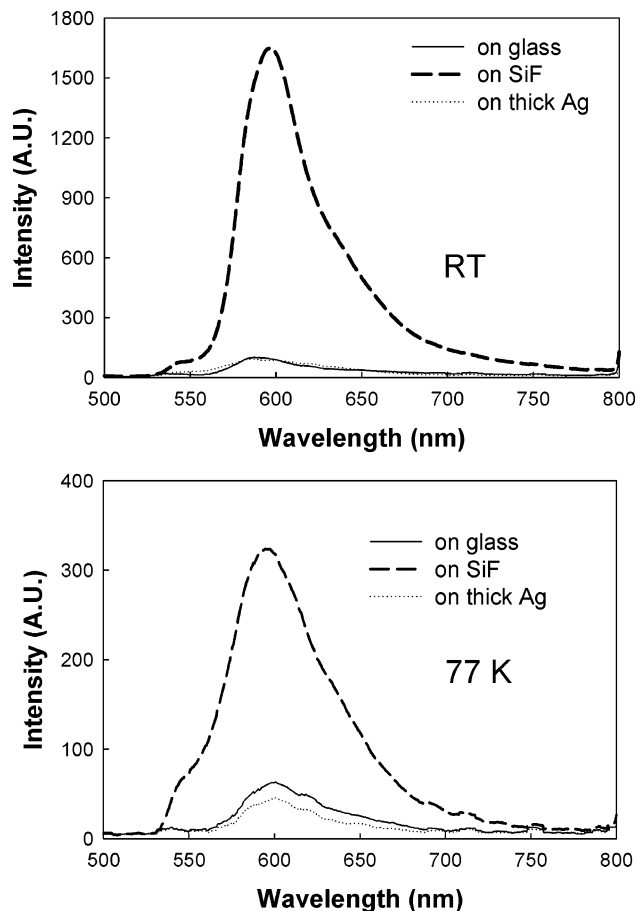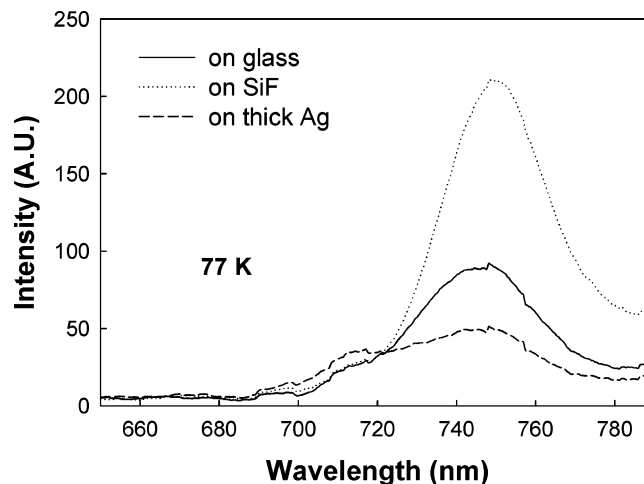

Figure 9. Phosphorescence spectra of Rose Bengal dried directly onto glass, SiFs, and a thick continuous silver film at 77 K. $\lambda_{ex} = 532$ nm.

Figure 8. Fluorescence emission spectra of RB dried directly on glass, SiFs, and a thick continuous silver film at both room temperature and 77 K (top and bottom, respectively). $\lambda_{ex} = 532$ nm.

In all of our applications of MEF to date, we have found that the enhanced fluorescence signals (quantum yields, Q_m) of fluorophores in close proximity (<10 nm) to metallic nanostructures could be well described by the following equations:[20]

$$Q_m = (\Gamma + \Gamma_m)/(\Gamma + \Gamma_m + k_{nr}) \qquad (7)$$

where Γ is the unmodified radiative decay rate, Γ_m is the metal-modified system radiative decay rate, and k_{nr} is the nonradiative rate. Similarly, the metal-modified lifetime, τ_m, of a fluorophore is decreased by an increased radiative decay rate:

$$\tau_m = 1/(\Gamma + \Gamma_m + k_{nr}) \qquad (8)$$

These equations result in most unusual predictions for fluorophore−metal combinations. From eqs 7 and 8, we can see that as the value of the system Γ_m increases, the quantum yield Q_m increases, while the lifetime, τ_m, decreases. This is contrary to most observations in fluorescence where the free-space quantum yield, Q_0, and lifetime, τ_0, nearly always change in unison.[21] From Figure 1, a highly efficient coupling to surface plasmons, where the plasmons efficiently and quickly radiate the coupled emission, results in a reduced fluorophore lifetime and enhanced observed emission intensity, cf., eqs 7 and 8.

3.4. Spin−Orbit Coupling. To further understand the observed enhancement in Rose Bengal fluorescence and phosphorescence emission, we studied RB dried directly onto glass, SiFs, and a continuous silver strip. This was necessary as spin orbit coupling[27] is known to enhance triplet yields and therefore potentially phosphorescence emission. For spin−orbit coupling with metals, the electron cloud overlap of both the metal and the fluorophore is required, cf., metal−ligand complexes;[27] hence drying RB solely on the surfaces may indicate whether any spin−orbit coupling is responsible, in part, for the enhanced phosphorescence signatures observed in Figure 4. In addition, surface plasmons cannot be generated in a continuous strip of metal (from the air side[9]) but can be in noncontinuous island films. Hence, no MEP would be expected for a continuous metal film unless spin orbit coupling was present to enhance the RB triplet yield.

Figure 7 shows the absorption spectra of Rose Bengal dried directly onto both glass and silvered glass. Much larger absorbance values at all wavelengths on SiFs were observed as compared to a suitable absorption blank. Table 4 also summarizes fluorescence and phosphorescence spectral data for Rose Bengal at RT and 77 K dried directly onto both glass and SiFs. It can be seen that the Rose Bengal fluorescence emission intensity ratio is increased in the dry condition, Table 4, as compared to that of Rose Bengal solution on SiFs, Table 1. At room temperature, the ratio changed from 3.2 (in solution, Table 1) to 5.4 (on dried surface, Table 4). At 77 K, the ratio changed from 5.7 (in solution, Table 1) to 16.4 (on dried surface, Table

25114 *J. Phys. Chem. B, Vol. 110, No. 49, 2006*

Zhang et al.

4). However, from Table 4, the Rose Begal MEP intensity ratio has decreased from 4.2 (in solution, Table 1) to 2.3 (on dried surface, Table 4), attributed to O_2 quenching; that is, no organic glass is present.

This surface contact MEF enhancement can be explained by a simple electromagnetic field enhancement,[10] observed many times for fluorophores very close to silver nanostructures, in addition to the MEF effect. This distance-dependent effect of MEF has been described by the authors previously.[24] In this case, the fluorophore undergoes enhanced excitation, as also evidenced by the enhanced absorption spectra shown in Figure 7.

It is interesting to compare both the fluorescence and the phosphorescence emission spectra of the RB dried on a continuous silver strip with those of both SiFs and bare glass, Figures 8 and 9. From Figure 8, we can clearly see that RB is quenched on the continuous silver surface, whereas SiFs show enhanced emission, Figures 2−4. In this regard, no surface plasmon-enhanced fluorescence would be expected in this geometry, but spin orbit coupling would be expected to be favorable for the continuous silver strip. Given that no enhanced emission is observed from the continuous surface, then spin orbit coupling is not thought to play any role in the enhanced luminescence signatures observed throughout this paper. In this regard, the phosphorescence emission can also be seen to be quenched on the silver surface, Figure 9.

4. Conclusions

In this paper, we have reported the observation of low-temperature metal-enhanced phosphorescence of Rose Bengal on SiFs. A 5-fold increase in phosphorescence intensity was observed as compared to an identical control sample containing no silver. We also observed that Rose Bengal displayed a much larger absorbance and emission intensity on SiFs, when it was directly dried onto SiFs. However, the emission is quenched when Rose Bengal is dried onto the continuous silver films, suggesting that spin−orbital coupling plays no role in the observed enhanced luminescence signals.

Metal-enhanced phosphorescence (MEP) may be of significance for phosphorescence-based clinical assays such as those used in photodynamic therapy. In addition, our finding suggests that photon-induced electronic excited states at low temperature can both induce and couple to surface plasmons facilitating both enhanced fluorescence, S_1, and phosphorescence, T_1, emission. The extent of enhanced triplet yields and the subsequent rates of singlet oxygen production of luminophores/fluorophores in close proximity to plasmonic structures, for potential downstream applications in photodynamic therapy, will be reported by us in due course.

References and Notes

(1) Dougherty, T. J.; Gomer, J. C.; Henderson, W. B.; Jori, G.; Kessel, D.; Lorbelik, M.; Moan, J.; Peng, Q. *J. Natl. Cancer Inst.* **1998**, *90*, 889.

(2) Raab, O.; Infusoria, Z. *Biol.* **1900**, *39*, 524.

(3) www.dermanetwork.org/information.

(4) Pass, H. I. *J. Natl. Cancer Inst.* **1993**, *85*, 443.

(5) Aslan, K.; Gryczynski, I.; Malicka, J.; Matveeva, E.; Lakowicz, J. R.; Geddes, C. D. *Curr. Opin. Biotechnol.* **2005**, *16*, 55.

(6) Geddes, C. D.; Aslan, K.; Gryczynski, I.; Malicka, J.; Lakowicz, J. R. Noble metal nanostructure for metal-enhanced fluorescence. *Review Chapter for Annual Reviews in Fluorescence in Fluorescence Spectroscopy*; Kluwer Academic/Plenum Publishers: New York, 2004.

(7) Geddes, C. D.; Aslan, K.; Gryczynski, I.; Malicka, J.; Lakowicz, J. R. Radiative decay engineering. *Topics in Fluorescence in Fluorescence Spectroscopy*; Kluwer Academic/Plenum Publishers: New York, 2005.

(8) Chowdhury, M. H.; Aslan, K.; Lakowicz, J. R.; Geddes, C. D. *Appl. Phys. Lett.* **2006**, *88*, 173104.

(9) Lakowicz, J. R. *Anal. Biochem.* **2004**, *324*, 153.

(10) Lakowicz, J. R. *Anal. Biochem.* **2001**, *298*, 1.

(11) Lakowicz, J. R.; Shen, Y.; D'Auria, S.; Malicka, J.; Fang, J.; Grcyzynski, Z.; Gryczynski, I. *Anal. Biochem.* **2001**, *301*, 261.

(12) Aslan, K.; Malyn, S. N.; Geddes, C. D. *Biophys. Res. Commun.* **2006**, *348*, 612.

(13) Lakowicz, J. R.; Malicka, J.; D'Auria, S.; Gryczynski, I. *Anal. Biochem.* **2003**, *320*, 13.

(14) Aslan, K.; Lakowicz, J. R.; Szmacinski, H.; Geddes, C. D. *J. Fluoresc.* **2005**, *15*, 37.

(15) Aslan, K.; Geddes, C. D. *Anal. Chem.* **2005**, *77*, 8057.

(16) Lakowicz, J. R. *Anal. Biochem.* **2005**, *337*, 171.

(17) Gryczynski, I.; Malicka, J.; Gryczynski, Z.; Lakowicz, J. R. *Anal. Biochem.* **2004**, *324*, 170.

(18) Geddes, C. D.; Gryczynski, I.; Malicka, J.; Lakowicz, J. R. *Photon. Spectra* **2004**.

(19) Zhang, Y.; Aslan, K.; Malyn, N. S.; Geddes, D. C. *Chem. Phys. Lett.* **2006**, *427*, 432.

(20) Aslan, K.; Leonenko, Z.; Lakowicz, J. R.; Geddes, C. D. *J. Fluoresc.* **2005**, *15*, 643.

(21) Lakowicz, J. R.; Shen, Y.; D'Auria, S.; Malicka, J.; Fang, J.; Gryczynski, Z. I.; Gryczynski, I. *Anal. Biochem.* **2002**, *301*, 261.

(22) Lakowicz, J. R.; Shen, Y.; Gryczynski, Z.; D'Auria, S.; Gryczynski, I. *Biochem. Biophys. Res. Commun.* **2001**, *286*, 875.

(23) Gryczynski, I.; Malicka, J.; Shen, Y.; Gryczynski, Z.; Lakowica, J. R. *J. Phys. Chem. B* **2002**, *106*, 2191.

(24) Geddes, C. D.; Lakowicz, J. R. *J. Fluoresc.* **2002**, *12*, 121.

(25) Aslan, K.; Lakowicz, J. R.; Geddes, C. D. *Anal. Bioanal. Chem.* **2005**, *382*, 926.

(26) Lakowicz, J. R. *Principles of Fluorescence Spectroscopy*; Kluwer Academic/Plenum Publishers: New York, 1999.

(27) Geddes, C. D. *Meas. Sci. Tech.* **2001**, *12*, R53.